Int. J. New. Chem., 2019, Vol. 6, Issue 2, pp. 109-132.

International Journal of New Chemistry
Published online 2019 in http://www.ijnc.ir/.

Online ISSN 2383-188X
Open Access

Original Research Article

The AIM, NBO thermodynamic, and quantum study of the interaction nitramide molecule with pristine, B, As and B&As doped of AlNNTs

Sedigheh Azadi doureh and Mahdi Rezaei–Sameti*

Department of Applied Chemistry, Faculty of Science, Malayer University, Malayer, 65174, Iran

*Corresponding author Fax number: mrsameti@gmail.com , mrsameti@malayeru.ac.ir

ABSTRACT

In this work, by using density functional theory, the adsorption of Nitramide (NH_2NO_2) molecule on the surface of pristine, B, As and B&As doped (4,4) armchair aluminum nitride nanotube (AlNNTs) is investigated. From optimized structures the adsorption energy, deformation energy, natural bond orbital (NBO), atom in molecule (AIM), quantum parameters, reduced density gradient (RDG) and molecular electrostatic potential (MEP) are calculated. The calculated results indicate that the adsorption energy values of NH_2NO_2 on the surface of pristine, As, B and B&As doped AlNNTs complex are negative and favorable in viewpoint of thermodynamic. Moreover the adsorption of NH_2NO_2 molecule on the surface of B&As doped AlNNTs is more stable and favorable than other models. It is notable that with doping B&As atoms in AlNNTs the deformation energy of NH_2NO_2 and nanotube are less than other models. The results of AIM and RDG outcomes demonstrate that nature of binding NH_2NO_2…AlNNTs is covalent bond type, indicates strong interactions. The results of NBO & Mullikan partial charge transfer, HOMO-LUMO, total charge transfer parameters (ΔN) and molecular

electrostatic potential (MEP) display that the charge transfer occurred from NH_2NO_2 molecule toward nanotube surface and electrical properties of system change significantly from original state. The results of this study reveal that the B&As doped AlNNTs is a good adsorbent for NH_2NO_2 molecule.

Keywords: Nitramine, B, AS, B&As doped, AlNNTs, DFT, AIM, NBO

Introduction

Shortly after successful discovery and synthesis of carbon nanotubes [1–3], intensive attentions have been dedicated to discovery and synthesis non-carbon nanotubes from the third and fifth group elements, which are neighbors of carbon in the periodic table, are an interesting subject of many researches [4–8]. One of them is Aluminum nitride nanotube (AlNNTs). The results of Zhang et al. indicated that AlNNTs in a hexagonal network is energetically favorable with sp^2 hybridization for both N and Al atoms [9]. Tondare et al., and Wu et al., [10–11] synthesized successfully the AlNNTs through different methods, the results of these study demonstrate that the electronic properties and semiconductor behavior of AlNNTs is independent of length, tubular diameter and chirality. The results of other studies reveal that the one-dimensional nanostructures of AlN have several unique properties such as high thermal conductivity at low temperature, high electrical resistivity, a moderately low dielectric constant, high dielectric breakdown strength, low thermal expansion coefficient close to the one of silicon, good mechanical strength, excellent chemical stability, and nontoxicity [12–13]. Aluminum nitride (AlN) nano materials are widely used in technological applications, mainly in micro and optoelectronics, such as laser diodes and solar-blind ultraviolet photodetectors and semiconductors [14–15]. Tuning the electronic structures of the semiconducting AlNNTs for specific application is evidently important in building specific electronic and mechanical devices

[16–18]. Adsorption of chemical species affects the electrical properties of AlN materials and it is a fundamental interest in development of potential electronic sensors [19–20]. The charge transfer between the nanotube and the adsorbate can increase or decrease the carrier density in semiconducting sheets, and thus significantly affects the electrical conductance of the material. Based on these observations, several groups have suggested the application of AlN sheets as promising gas sensors [21]. Rastegar et al. have recently showed that an AlN sheet can detect low concentration of NO_2 in the presence of NH_3 [21]. So far, adsorptions of some gaseous molecules including NH_3, H_2, N_2, CO, formaldehyde and CO_2 on the AlNNTs have been reported [22–26]. These studies showed that the pristine type of the AlNNTs is not sensitive toward NH_3 and CO molecules. Other research indicated that O-doped AlNNTs would be a potential candidate for NH_3 molecule detection [27]. The potential possibility of single-walled pristine AlNNTs as a gas sensor for SO_2 molecule detection is confirmed that the adsorption energy of SO_2 molecule is not so large to hinder the recovery of AlNNTs and therefore the sensor will possess short recovery times [28]. The results of Ahmadi Peyghan et al. and Baei et al.[29–31] indicated that the electric field effect increase the electrical and sensivity of AlNNTs toward to CO and O_2 molecules. Beheshtian et al. [32–38] investigated the interaction and adsorption of H_2, hydrogen cyanide, nitrous oxide, CO gas, sulfide dioxide, nitrogen dioxide and H_2S gas on the surface of the pristine and doped models of AlNNTs. These results confirmed that AlNNTs could selectively detect this gas in the presence of other molecules. Seif et al. [39] results confirm that the chemical shielding (CS) parameters for the O-decorated AlNNTs at the sites of various ^{27}Al and ^{15}N atoms alter significantly from pristine models. The computational results of Raissi et al. [40] showed that $COCl_2$ molecule adsorbed on the pristine AlNNTs through weak van der Waals interaction, which means that the adsorption is physisorption

process. Nitramide is a chemical compound with the molecular formula H_2NNO_2. Nitramide derivatives are widely used as explosives examples include RDX and HMX in military explosive, propellant and fuel applications. In last years, extensive theoretical and experimental have been applied to study the interaction of NH_2NO_2 compound with nanomaterial and nanotubes [41–42]. In the previous study we found that the adsorption energy of NH_2NO_2 molecule on the surface of pristine and Ni functionalized GaNNTs is in range –6.59 to –48.16 Kcal/mol and is physisorption type [43]. On the other work we found that the adsorption process of nitramide molecule on the exterior surface of pristine and C-replaced BN nanosheet is exothermic and the deformation energy results displayed that the geometry and structure of BN nanosheet and nitramide in the BN nanosheet/NH_2NO_2 complex change significantly from the original state [44]. Following our pervious studied [45–46], the main objective of this work is to investigate the adsorption and interaction of NH_2NO_2 molecule on the surface of pristine and B&As doped AlN nanotube. The considered adsorptions models of NH_2NO_2 molecule from H and O head on the surface of nanotube is named with a and b indexes and the pristine, B, As and B&As doped AlNNTs is defined with A, B, C and D models. The structural, chemical reactivity, quantum parameters, adsorption energy, deformation energy, reduced density gradient (RDG), atom in molecule (AIM) and molecular electrostatic potential (MEP) parameters for all selected models are calculated. The obtained results can be useful to examine the performance of AlNNTs to detect and adsorb of nitramine molecule.

Computational section

In this study the selected models of A-a, A-b, B-a, B-b, C-a, C-b, D-a and D-b adsorption models on the surface of pristine, B, As and B&As doped models are optimized by using density functions theory at the B3LYP/6-31G(d, p) level of theory with performing the GAMESS suite

of programs [47–48]. The optimization criteria (Max. force= 0.00022, RMS force= 0.00032, Max displacement =0.0002 and RMS displacement= 0.0008) and in here, there is no imaginary vibrational frequency.

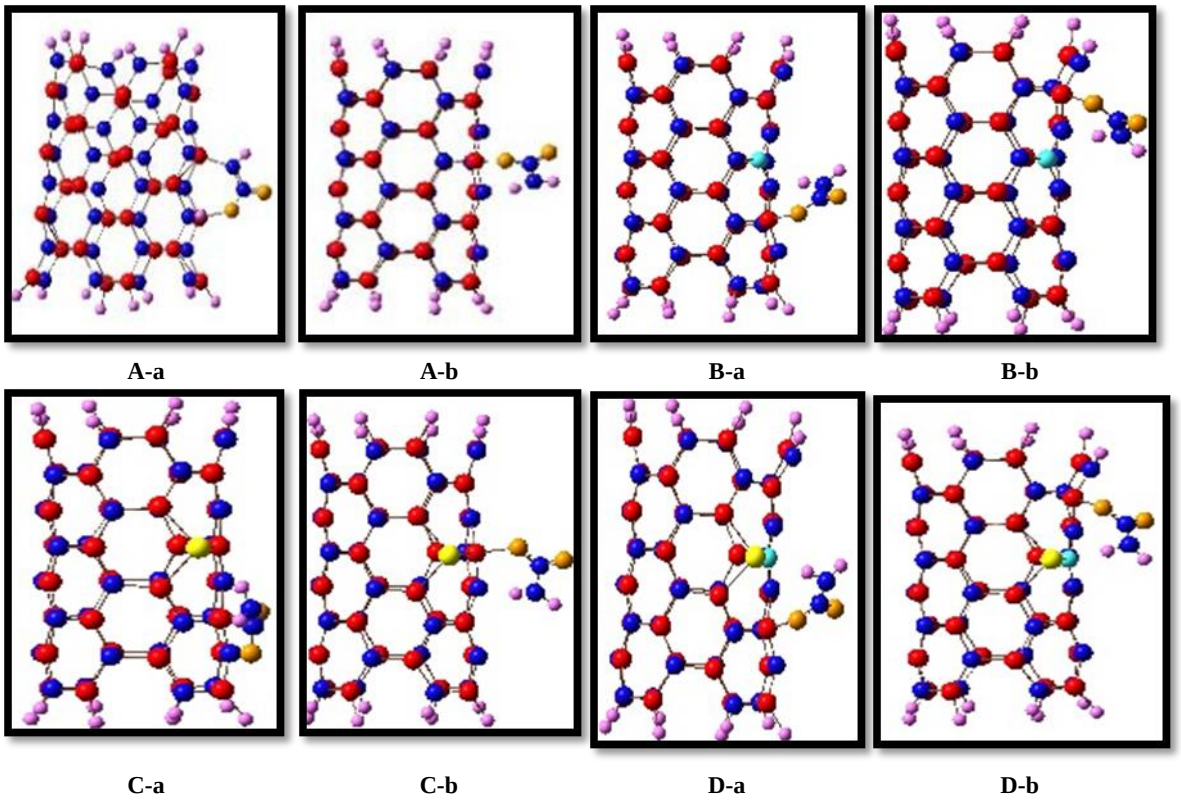

Fig. 1 2D views of (NH_2NO_2) molecule on the surface of pristine, B, As and B&As doped (4,4) armchair AlNNTs for A-a to D-b adsorption models

The optimized results are given in Fig. 1, at all models, for preventing the dangling bonds at the edges of the nanotube the ends of the nanotube are saturated by hydrogen atoms. The adsorption energy (E_{ads}) and thermodynamic parameters involve (ΔH, ΔS and ΔG) for NH_2NO_2 adsorption on the surface of the pristine and B, As, B&As doped AlNNTs are calculated by Eq. (1):

$$\Delta M = M_{AlNNTs/NH2NO2} - (M_{AlNNTs} + M_{NH2NO2r}) + BSSE \qquad M: E_{ads}, G, S, H \qquad (1)$$

where $M_{AlNNTs\text{-}NH2NO2}$ is the total energy and thermodynamic parameters of the complex consisting of NH_2NO_2 gas and AlNNTs, while M_{AlNNTs} and M_{NH2NO2} are the total energies and

thermodynamic parameters of AlNNTs and NH_2NO_2 respectively. The BSSE is basis set superposition errors. For all adsorption models the BSSE values energy are in range 0.0002 to 0.014 Kcal/mol and all calculated energy are corrected. The HOMO (highest occupied molecular orbital) and LUMO (lowest unoccupied molecular orbital) are calculated at the above level of theory. HOMO is an electron donor and LUMO can accept electrons. By using the HOMO and LUMO energies, the quantum descriptive involve gap energy (E_{gap}), electronic chemical potential (μ), global hardness (η) and charge transfer parameters (ΔN) [40–44] are calculated at the above level of theory (see Eqs 2-5), and obtained results are listed in Table 1.

$$E_{gap} = E_{LUMO} - E_{HOMO)} \quad (2)$$

$$\mu = \frac{E_{HOMO} + E_{LUMO}}{2} \quad (3)$$

$$\eta = \frac{E_{LUMO} - E_{HOMO}}{2} \quad (4)$$

$$\Delta N = -\frac{\mu}{\eta} \quad (5)$$

These parameters reflect the reactivity, conductivity, and optical properties of the molecule. A molecule having small gap energy is more polarizable and is generally associated with a high chemical reactivity and low kinetic stability.

Results and discussion

Adsorption properties and thermodynamic parameters

The optimized structures of the A-a, A-b, B-a, B-b, C-a, C-b, D-a and D-b adsorption models are presented in Fig. 1. The calculated average Al–N bond lengths of the pristine, B, As and B&As doped AlNNTs are 1.47, 1.45, 2.40 and 2.15 Å respectively (see Table S1 in the supplementary data), this result is in good agreement with the other reports [28–33]. To examine the adsorption properties of NH_2NO_2 molecule on the surface of pristine, B, As and B&As doped AlNNTs, the adsorption energies and thermodynamic parameters for all considered

models are calculated using Eq. 1. The calculated adsorption energies and thermodynamic parameters of NH_2NO_2/nanotube complex are summarized in Table 1.

Table 1 Thermodynamic parameters (Kcal/mol), adsorption energy(Kcal/mol), deformation energy(Kcal/mol), solvent effect parameters (Kcal/mol) and dipole moment ((Debye) of NH_2NO_2 adsorption on the surface of pristine and B, As and B&As doped AlNNTs Models A, B, C and D

	A-a	*A-b*	*B-a*	*B-b*	*C-a*	*C-b*	*D-a*	*D-b*
E_{ads}	-32.02	-31.74	-33.48	-34.88	-34.88	-34.71	-35.40	-36.11
$E_{def\ (AlNNTs)}$	-7.96	-7.96	-7.96	-9.18	-9.18	-6.96	-5.26	-5.81
$E_{def\ NH2NO2}$	-6.20	-8.54	-6.26	-7.99	-7.99	-3.90	-0.87	-1.09
$E_{bin\ complex}$	-49.80	-48.24	-47.71	-52.07	-52.07	-38.57	-41.53	-43.02
ΔG	-19.25	-18.51	-20.45	-22.97	-18.67	-19.38	-19.62	-21.16
ΔH	-31.02	-30.05	-32.67	-34.57	-30.90	-29.23	-32.79	-33.96
Δμ	4.84	4.61	4.94	4.93	4.78	4.17	4.73	4.74
$\Delta G_{solvation}$	25.09	22.27	24.61	27.23	23.36	22.08	23.85	25.24

Based on the calculated results, it has been found that the adsorption energy for all adsorption models are negative, which means that the adsorption process is favorable and spontaneous. Inspection of results confirm that the adsorption energy of D-a and D-b models when the NH_2NO_2 molecule vertically approaches to the outer surface of nanotube with H and O heads, is more stable than other models. These results suggest that with doping B and As atoms the adsorption of NH_2NO_2 molecule on the surface of AlNNTs increase significantly from privative models and adsorption process are more favorable than pristine models. On the other hand the dipole moment of NH_2NO_2/nanotube complex in all models is in range 4.17 to 4.94 Debye and alter slightly with adsorbing NH_2NO_2 molecule. The recovery time of the sensor device based on the conventional transition state theory is calculated by Eq. 6.

$$\tau = \nu_0^{-1} \exp^{(-Ead/kT)} \quad (6)$$

where T is temperature, k is the Boltzmann's constant, and ν_0 is the attempt frequency. According to this equation, the average recovery time of A-a, B-a , C-a and D-a models are 2.07×10^{11} , 2.42×10^{12} , 2.53×10^{13} and 6.05×10^{13} s respectively. These results demonstrate that the interaction between nanotube and NH_2NO_2 molecule at all models is strong, and the pristine,

B, As and B&As doped AlNNTs is suitable for making adsorbent of NH_2NO_2 molecule. The recovery time for A-a model is lower than those other models and so the interaction and adsorption of NH_2NO_2 molecule on the pristine surface of AlNNTs is weaker than those other models. To better investigate the adsorption properties NH_2NO_2 molecule on the surface of pristine, B, As and B&As doped AlNNTs, the deformation energy (E_{def}) of NH_2NO_2, nanotube and NH_2NO_2/ nanotube for all adsorption models are calculated by using Eqs (7-9):

$$E_{def\ AlNNTs} = E_{AlNNTs\ in\ complex} - E_{AlNNTs} \quad (7)$$

$$E_{def\ NH_2NO_2} = E_{NH_2NO_2 in\ complex} - E_{NH_2NO_2} \quad (8)$$

$$E_{\text{int}} = E_{nanotub/NH_2NO_2 complex} - E_{AlNNTs\ in\ complex} - E_{NH_2NO_2 in\ complex} \quad (9)$$

here the $E_{AlNNTs\ in\ complex}$ and $E_{NH2NO2\ in\ complex}$ are the total energy of AlNNTs and NH_2NO_2 in the NH_2NO_2/AlNNTs complex, when NH_2NO_2 and AlNNTs are absent oneself respectively. The E_{int} is interaction energy for NH_2NO_2/AlNNTs complex. Based on the calculated results of Table 1, the deformation energy values of the nanotube and NH_2NO_2 molecule at the all adsorption models are negative. The negative values of deformation energy indicate that the molecular deformation is spontaneous and the molecular structures of compound change spontaneously from original state. The deformation energy of nanotube in the B-b (–9.18 Kcal/mol) and C-a (–9.18 Kcal/mol), are more negative than other models and so the deformed structure in these models are more stable than other models. The deformation energy of NH_2NO_2 molecules in the A-b model (–8.54 Kcal/mol) is more than other models. It is notable that with doping B& As atoms in the D-a and D-b models the deformation energy of NH_2NO_2 molecule are less than other models. Which means the curvature in the geometry of NH_2NO_2 in the As&B doped AlNNTs/NH_2NO_2 complex is significantly smaller than other system. Thus, the As&B doped AlNNTs can better protect the geometries of NH_2NO_2 compared to pristine, B and As doped AlNNTs. On the other hand, comparing deformation energy of NH_2NO_2 and nanotube indicate

that the curvature in the structure NH_2NO_2 and nanotube at all adsorption models are almost the same. The thermodynamic parameters involve enthalpy (ΔH), Gibbs Free energy in gas phase (ΔG)and Gibbs Free energy in water phase ($\Delta G_{solvation}$) for adsorption of NH_2NO_2 molecule on the surface of pristine, B, As and B&As doped AlNNTs are calculated by Eq. 1 and results are listed in Table 1. As displayed in Table 1, the ΔH, and ΔG values for all adsorption models are negative. Comparison results indicate that the ΔH, and ΔG values for all adsorption models in range (–29.23 to –33.96) and (–18.51 to –22.97) Kcal/mol respectively. The enthalpy and Gibbs free energy value of B-b model is more than other models and the adsorption of NH_2NO_2 in this model is more exothermic and spontaneous than other models. The infra–red (IR) spectrum of all adsorption models are determined from output of thermodynamic calculation, and the calculated results are given in the Fig S1 in supplementary data. Comparison the IR spectrum of all adsorption models show that the maximum epsilon (intensity of peak) each spectrum is shown in the frequency 1000 cm^{-1} and with doping B, As and B&As atoms the altitude of the maximum epsilon increase significantly from pristine model due induction effect of the doping atoms. On the other hand, when adsorption of NH_2NO_2 is investigated in an aqueous medium, the results indicate that the amount of Gibbs free energy in this system is positive, and the adsorption of NH_2NO_2 on the surface of pristine, B, As and B&As doped AlNNTs is unspontaneous in thermodynamic approach. Comparison results indicate that the $\Delta G_{solvation}$ of the A-a (pristine model) and D-b model (B&As-doped) is more than other models and adsorption of NH_2NO_2 on the surface of nanotube in these models are more unfavorable than other models.

The HOMO and LUMO orbitals and quantum descriptors

One of the most important terms in the study of interaction NH_2NO_2 with nanotube is the highest occupied molecular orbital (HOMO) and lowest unoccupied molecular orbital (LUMO) and related quantum parameters. The HOMO and LUMO orbitals density for all adsorption models are displayed in Fig 2.

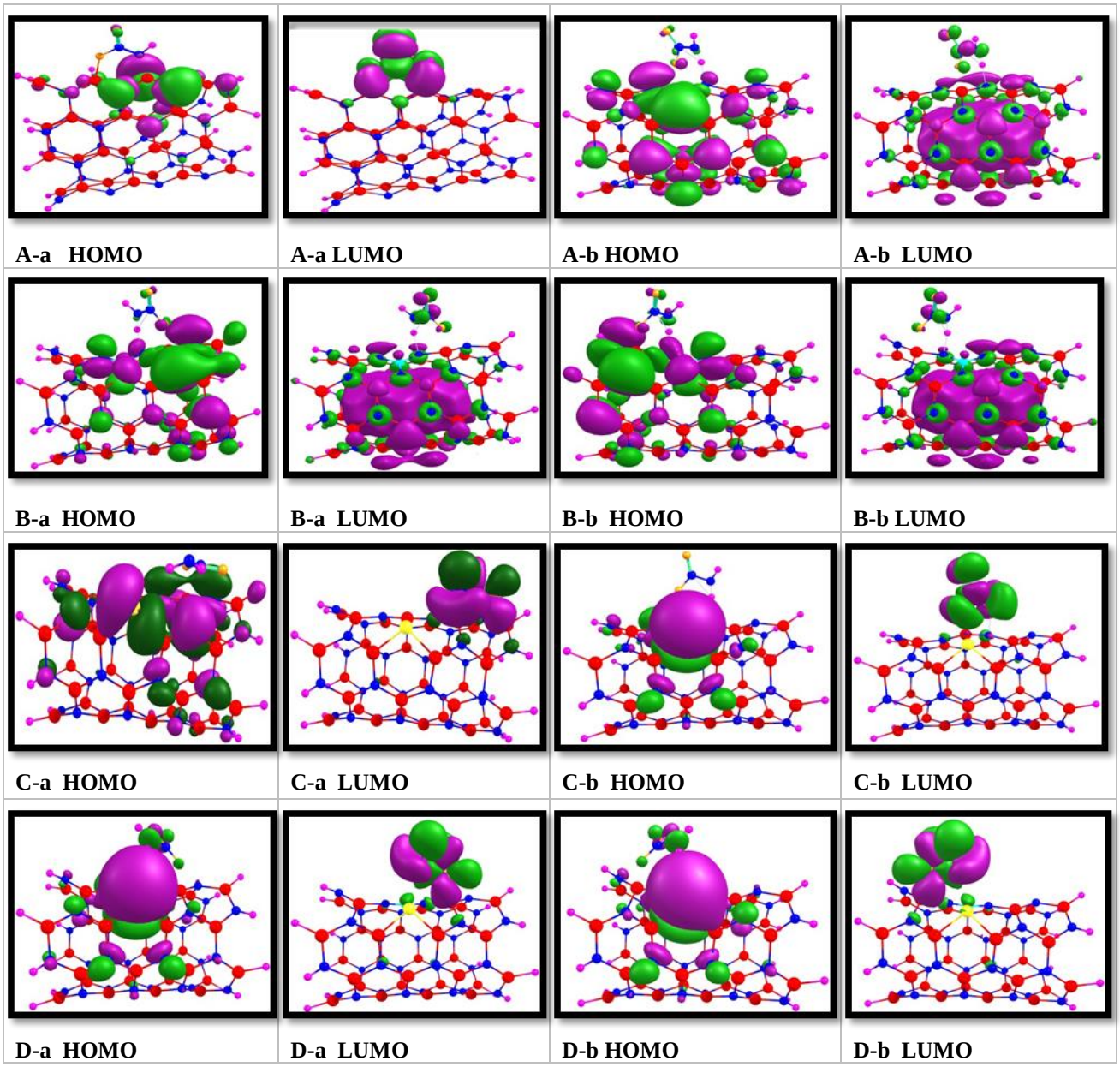

Fig. 2 The HOMO-LUMO orbital distribution of (NH_2NO_2) molecule on the surface of pristine, B, As and B&As doped (4,4) armchair AlNNTs for A-a to D-b adsorption models

Inspection of outcomes indicate that the HOMO orbital density at the all adsorption models are distributed around nanotube surface specially around adsorption position area. Whereas the LUMO orbital density is localized around NH_2NO_2 molecule. The most density of LUMO orbital in the A-b, B-a and B-b models has distributed throughout the nanotubes in the adsorption region. As result, the surface of the nanotube is a good place to attack electrophilic species and the surface of NH_2NO_2 molecule is a good place to attack nucleophilic species. However in the nanotube/NH_2NO_2 complex a significant overlap and electron density transfer can be performed between the HOMO orbital of NH_2NO_2 and the LUMO of nanotube. These results agree with the results of the NBO ($\Delta\rho_{NBO}$) and Mulliken ($\Delta\rho_{Mulliken)}$ partial charge transfer, charge transfer parameters (ΔN) and the adsorption energy (see Table 2). The positive values of $\Delta\rho_{NBO,}$ $\Delta\rho_{Mulliken}$ and ΔN in Table 2 demonstrate that the charge transfer occurs toward nanotube. Noticeably, the charge transfer between NH_2NO_2 molecule and nanotube of D-a and D-b (B&As doped) models with $\Delta N \approx 1.61$, $\Delta\rho_{Mulliken} \approx 0.16$ |e| and $\Delta\rho_{NBO} \approx 0.13$ |e| which are more than other adsorption models. From these results, it can be suggested that the stabilization of the NH_2NO_2/nanotube complex is mainly governed by electrostatic interactions.

From HOMO and LUMO energy the quantum descriptor are calculated, these parameters are used to establish correlation in various chemical and biochemical systems and to characterize the chemical reactivity and kinetic stability of the molecule [49–51].

Table 2 Quantum parameters and Mulliken &NBO charge of NH_2NO_2 adsorption on the surface of pristine and B, As and B&As doped AlNNTs Models A, B,C and D

	A-a	*A-b*	*B-a*	*B-b*	*C-a*	*C-b*	*D-a*	*D-b*
E_{HOMO}/eV	-7.89	-7.58	-7.82	-7.82	-7.30	-7.72	-7.28	-7.33
E_{LUMO}/eV	-1.38	-1.22	-1.42	-1.39	-1.40	-1.75	-1.71	-1.70
Egap/eV	6.51	6.22	6.41	6.43	5.90	5.97	5.57	5.63
μ/eV	-4.63	-4.40	-4.62	-4.61	-4.35	-4.74	-4.50	-4.51
η/eV	3.25	3.18	3.20	3.22	2.95	2.99	2.78	2.81
$E_{FL/eV}$	-4.63	-4.40	-4.62	-4.61	-4.35	-4.76	-4.50	-4.51
(Δϕ)/eV	4.63	4.40	4.62	4.61	4.35	4.76	4.50	4.51
ΔN	1.42	1.38	1.44	1.43	1.47	1.58	1.61	1.60
$\Delta\rho_{Mulliken}$	0.08	0.03	0.08	0.08	0.10	0.17	0.16	0.16
$\Delta\rho_{NBO}$	0.04	0.23	0.04	0.05	0.07	0.14	0.12	0.13

The calculated gap energy between HOMO and LUMO energies is listed in Table 2, and the density of state graph of NH_2NO_2/nanotube system for all models are shown in Fig. 3. The density of states (DOS) of a system describes the number of states per interval of energy at each energy level that are available to be occupied by electrons.

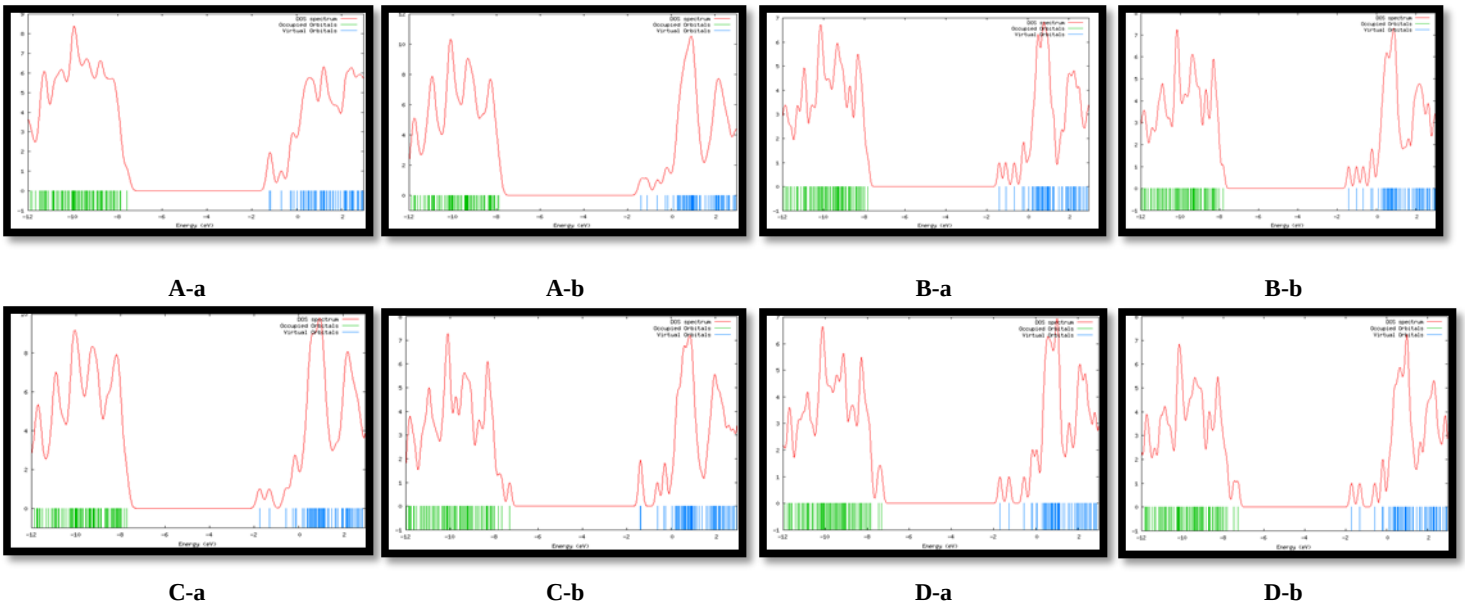

Fig. 3 The DOS plots of (NH_2NO_2) molecule on the surface of pristine, B, As and B&As doped (4,4) armchair AlNNTs for A-a to D-b adsorption models

A high DOS at a specific energy level means that there are many states available for occupation. A DOS of zero means that no states can be occupied at that energy level. In general, a DOS is an average over the space and time domains occupied by the system. The DOS plots of all

adsorption models are calculated at the –12 to 5 eV (see Fig . 3). Comparison results indicate that the number of DOS peaks with doping B atom at B-a, B-b models and D-a and D-b models is more than pristine and As doped AlNNTs. These results confirm that doping B atom and adsorbing NH_2NO_2 molecule is caused a significant change in the characteristic features of the DOS. On the other hand, the gap energy between HOMO and LUMO orbitals in range 5.57 to 6.51 eV. With doping B&As atoms the gap energy decrease significantly from original values and this result demonstrates a considerable changes has occurred. Moreover, when the NH_2NO_2 molecule adsorbs on the surface of B&As doped AlNNTs, the global hardness and electrical potential of the system are significantly decreased indicating that the reactivity of the system is increased. Comparison results indicate that the reactivity and conductivity of NH_2NO_2/nanotube system decrease in order: A-a> B-a>C-a>D-a and these results in agreement with adsorption thermodynamic parameters. These outcomes clearly show that with doping B, As and B&As increase the sensivity of AlNNTs to adsorb and detect of NH_2NO_2 molecule.

To gain more insight into conductivity and charge transfer between NH_2NO_2 and nanotube in the A-a, A-b, B-a, B-b, C-a, C-b, D-a and D-b models the Fermi level energy (E_{FL}) of system and calculated values are given in Table 2. The E_{FL} of all adsorption models is in range –4.35 to –4.76 eV. The variations of Fermi level energies reveal that a remarkable number of electrons transfer during the interaction between nanotube and NH_2NO_2 molecule, as results the electronic properties of system change significantly from original state, which significantly affected the electrical conductance of system.

The work function parameters ($\Delta\phi$) of systems are calculated using follow equation:

$$\Delta\phi = E_{\inf} - E_{FL} \quad (10)$$

here E_{inf} is the electrostatic potential at infinity and E_{FL} is the Fermi level energy. In this consideration, the electrostatic potential at infinity is assumed to be zero. As known, the work

function parameter of a system is the least amount of energy required to remove an electron from the Fermi level to a point far enough not to feel any influence from the material [52]. The emitted electron current densities in a vacuum are theoretically described by the following classical equation:

$$j = AT^{2}\exp^{(-\Delta\phi/kT)} \quad (11)$$

where A is called the Richardson constant (A/m^2), T is the temperature (K). The work function values for A-a, B-a, C-a and D-a adsorption models are 4.63, 4.62, 4.35 and 4.50 eV (see Table 2). According to eq. 11 the emitted electron current density of system is exponentially related to the negative value of $\Delta\phi$. Comparison results reveal that the work function of As and B&As doped AlNNTs is lower than pristine and B doped and so the emitted electron current densities of C-a and D-a adsorption models is more than A-a and B-a models. It may be conclude that , the dipole moment of As and B&As doped AlNNTs is more than pristine and B doped, thereby the dipole moment these systems is more than pristine and B doped and these results are significantly in agreement with adsorption energy, conductivity of system.

Atom in molecule method

To further understand, the bonding navigate between NH_2NO_2 and nanotube and electrical properties of between them, the electron densities (ρ) and Laplacian of electron, densities ($\bigtriangledown^2\rho$) at bond critical point (BCP), the potential energy (V_{BCP}), the total electronic energy (H_{BCP}), and the kinetic energy (G_{BCP}) of the bond in critical points are calculated using AIMALL program [53–54]. The calculated results are given in Table 3.

Table 3 The atom in molecule (AIM) parameters of NH_2NO_2 adsorption on the surface of pristine and B, As and B&As doped AlNNTs Models A, B, C and D

	ρ	$\nabla^2\rho$	G	H	V
A-a	0.0531	-0.0773	0.0756	-0.0169	0.0739
A-b	0.0498	-0.0811	0.0765	-0.0046	0.0718
B-a	0.0488	-0.0803	0.0751	-0.0052	0.0698
B-b	0.0413	-0.0861	0.0804	-0.0057	0.0747
C-a	0.0418	-0.0640	0.0606	-0.0033	0.0572
C-b	0.0451	-0.0701	0.0665	-0.0036	0.0628
D-a	0.0448	-0.0714	0.0669	-0.0044	0.0625
D-b	0.0459	-0.0742	0.0693	-0.0048	0.0645

As known, the negative values of $\bigtriangledown^2\rho$ and H_{BCP} refer to strong interaction (strong covalent bond), the positive values of $\bigtriangledown^2\rho$ and H values denote the weak covalent interactions (strong electrostatic bond) and the positive value of $\bigtriangledown^2\rho$ and negative value of H_{BCP} define medium strength as partially covalent bond. According to outcomes of table 3, the values of $\bigtriangledown^2\rho$ and H_{BCP} for all adsorption models is negative and refers to strong interaction (strong covalent bond). These results demonstrate that the bonding navigate between nanotube and NH_2NO_2 molecule [(NH_2NO_2…pristine, B, As and B&As doped AlNNTs] is covalent bond type, indicates strong interactions.

Natural bond orbital

In this work, to investigate the charge transfer behavior between nanotube and adsorbent interaction we calculate the natural bond orbital (NBO) parameters [55]. This method is an effective tool to determine the chemical interpretation of hyper–conjugative interaction and electron density transfer from the filled lone pair electron. For this reason, the stabilization energy (E^2) associated with the delocalization between each donor (i) and acceptor (j) orbital is

determined by using Eq. 12:

$$E^{(2)} = q_i \frac{F_{ij}^2}{\varepsilon_j - \varepsilon_i} \quad (12)$$

where q_i is donor orbital occupancy, ε_i and ε_j are orbital energies and F_{ij} is the off–diagonal NBO Fock matrix element. The larger values of $E^{(2)}$ indicate, the strong interaction between electron donors and electron acceptors, and more donating tendency from electron donors to electron acceptors and the greater the extent of conjugation of the whole system. The calculated results for $E^{(2)}$ values and corresponded donor and acceptor orbitals for A-a, A-b, B-a, B-b, C-a, C-b, D-a and D-b adsorption models around of B, As and B&As doped position are listed in Table 4.

Table 4 The stabilization energy for donor and acceptor orbital of NH_2NO_2 adsorption on the surface of pristine and B, As and B&As doped AlNNTs Models A, B, C and D

Structure	Donor(i)	→	Acceptor(j)	E(2) (Kcal/mol)	E_j-E_i (a.u.)	F_{ij} (a.u.)
A-a	σ N32-Al42	→	σ*Al34-N32	6.14	0.90	**0.067**
A-b	σ N32-Al42	→	σ*Al34-N32	5.96	0.92	**0.066**
B-a	σ N32-Al42/B	→	σ*Al34-N32	3.55	1.05	**0.055**
B-b	σ N32-Al42/B	→	σ*Al34-N32	4.07	1.04	**0.059**
C-a	σ N32-Al42	→	σ*Al34-N32	6.15	0.95	**0.068**
C-b	σN42/As-Al32	→	σ*Al32-N31	5.67	0.67	**0.055**
D-a	σ N32-Al42/B	→	σ*Al34-N32	4.29	1.05	**0.034**
D-b	σ N32-Al42/B	→	σ*Al34-N32	4.46	1.09	**0.063**

The strong intramolecular hyper conjugative interaction of donor orbital to acceptor orbital for A-a, B-a, C-a and D-a occur in the $\sigma N_{32} - Al_{42} \rightarrow \sigma^* Al_{34} - N_{32}$. Inspection of results reveal that the order of $E^{(2)}$ value for adsorption of NH_2NO_2 from H site is: C-a>A-a>D-a> B-a and from O site is: A-b>C-b>D-b>B-b. These results demonstrate that, when NH_2NO_2 molecule from H site adsorbed on the surface of the As-doped AlNNTs and from O site adsorbed on the surface of the pristine AlNNTs the strongest charge transfer interaction is occurred between NH_2NO_2 molecule

and nanotube and so the electrical properties and adsorption energy of these forms are larger than other states. It is notable that with doping B atom in all adsorption models (B-a and B-b models) the $E^{(2)}$ values are lower than other those models and so the least charge transfer is occurred in them.

Molecular electrostatic potential (MEP)

To better understand of charge distribution around adsorption position, the molecular electrostatic potential (MEP) [56–57] plots for all adsorption models are calculated and result are shown in Fig. 4. Here to specify the different values of the electrostatic potential on the surface adsorption area a different colors are used.

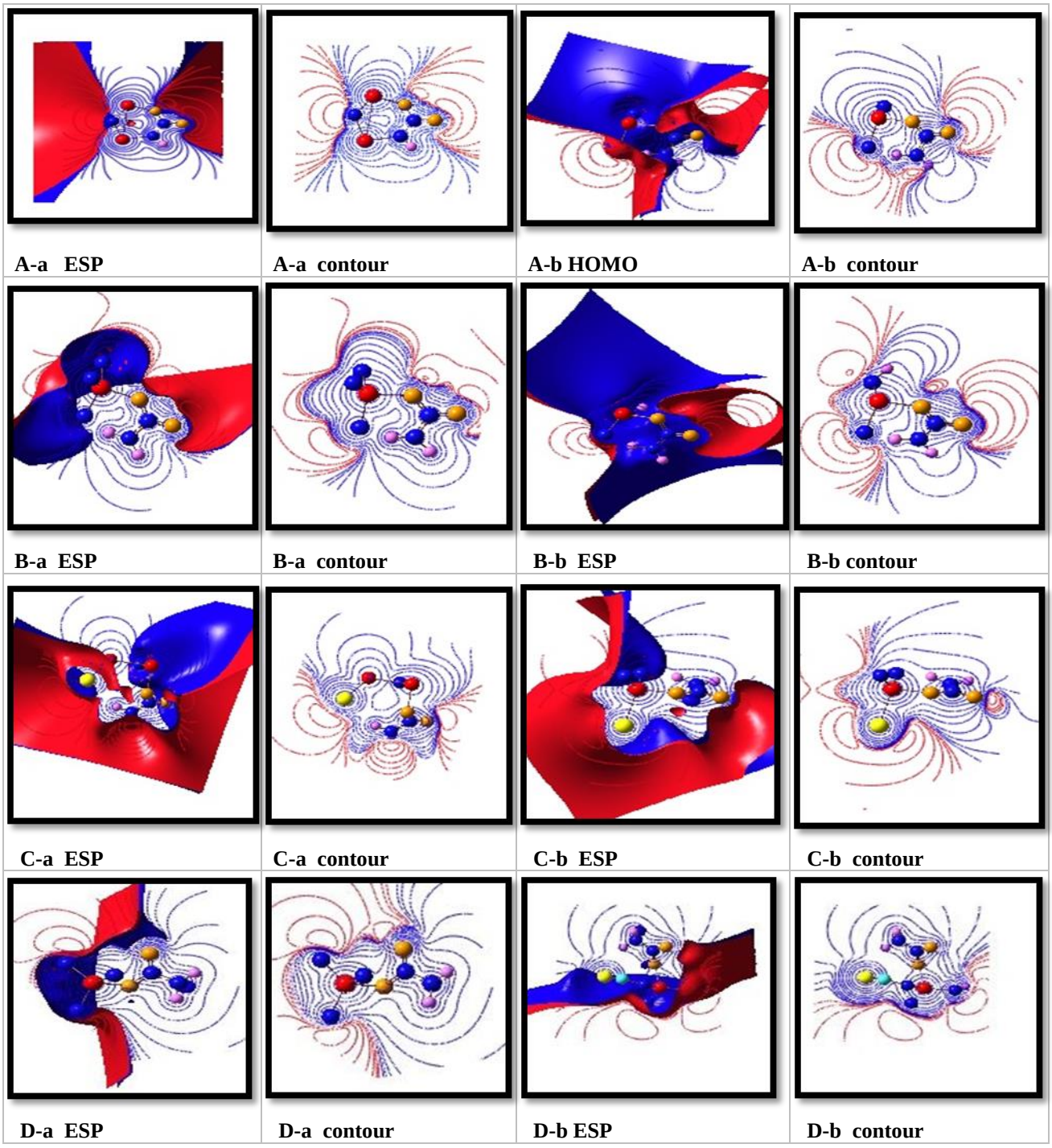

Fig. 4 The MEP Plots of (NH_2NO_2) molecule on the surface of pristine, B, As and B&As doped (4,4) armchair AlNNTs for A-a to D-b adsorption models

The blue color represents the positive charges distribution or the nucleophilic regions and the red color represents the negative charges distribution or the electrophilic regions. Based on the

outcomes in the A-a, A-b, B-a, B-b, C-a, C-b, D-a and D-b models a significant electron density, and negative potential, red color, are localized on the surface of nanotube and maximum positive electrostatic potential are observed around adsorption position and it is localized on the surface of NH_2NO_2 molecule. These results have a good agreement with NBO charge transfer, ΔN and quantum parameters. It can be clearly observed that in the B-b model with doping B atom the positive electrostatic potential around adsorption position is more than other models.

Reduced density gradient (RDG) and NCI index

One of the interesting methods to investigate the intramolecular interactions and evaluate the nature of the weak interactions is non–covalent interaction index (NCI) that it related to the non–covalent interaction and the reduced density gradient (RDG) is calculated by Eq. 13:

$$RDG(r) = \frac{1}{2(3\pi^2)^{1/3}} \frac{|\nabla\rho(r)|}{\rho(r)^{4/3}} \quad (13)$$

Non–covalent interactions are characterized by small values of RDG. These isosurface expand over interacting regions of the complex. The product between electron density ρ(r) and the sign of the second lowest eigenvalues of electron density hessian matrix (λ_2) has been proposed as a tool to distinguish the different types of interactions. The scatter graphs of RDG versus sign(λ_2) ρ(r) for all adsorption models are shown in Fig. 5. The X–axis and Y axis are sign(λ_2)ρ(r) and RDG function respectively. The sign(λ_2)ρ(r) and NCI–RDG plots are obtained with Multiwfn program[58]. The sign (λ_2)ρ(r) is utilized to distinguish the bonded (λ_2<0) interactions from nonbonding (λ_2>0) interactions.

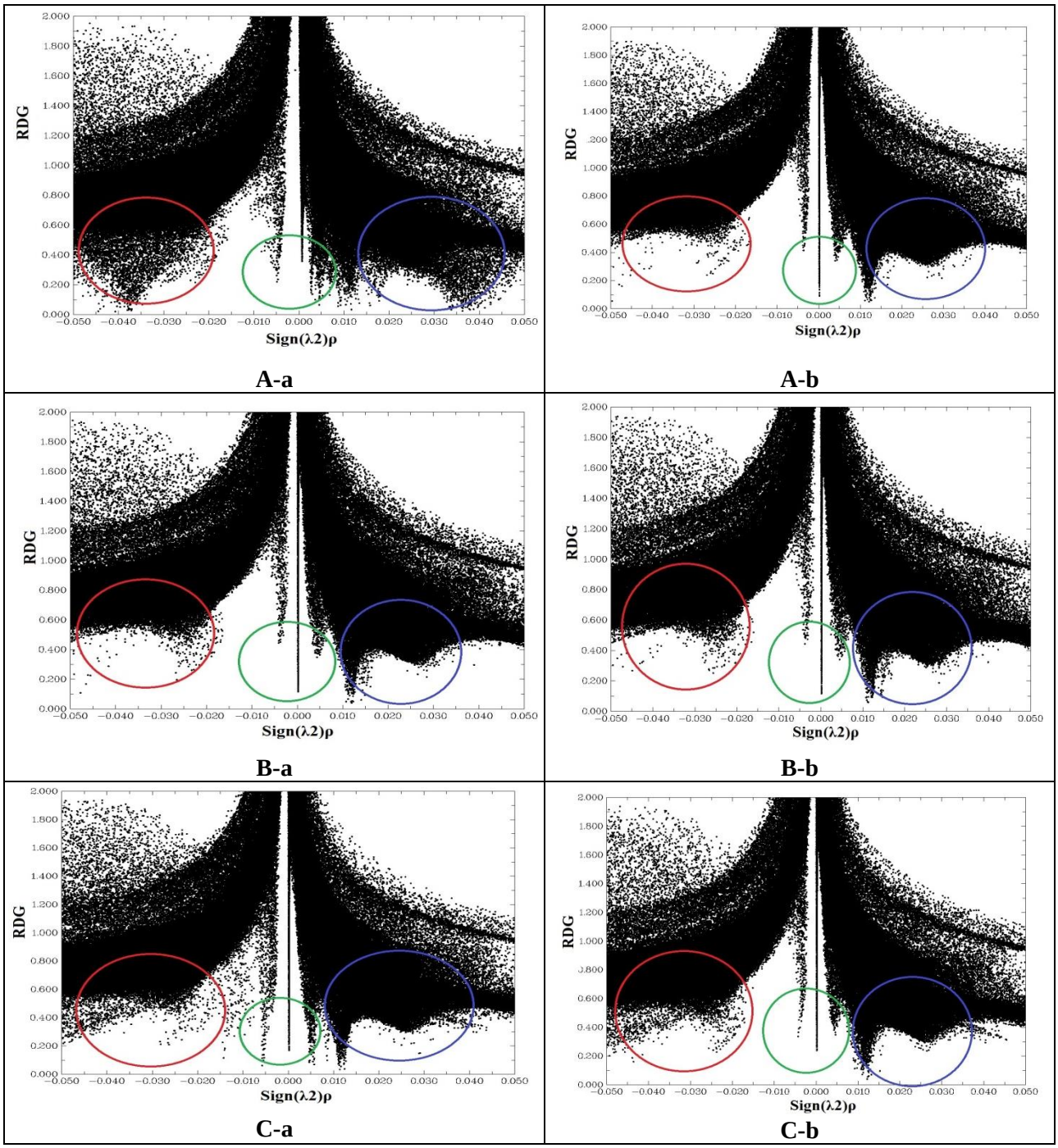
RDG
Sign(λ2)ρ
A-a
A-b
B-a
B-b
C-a
C-b

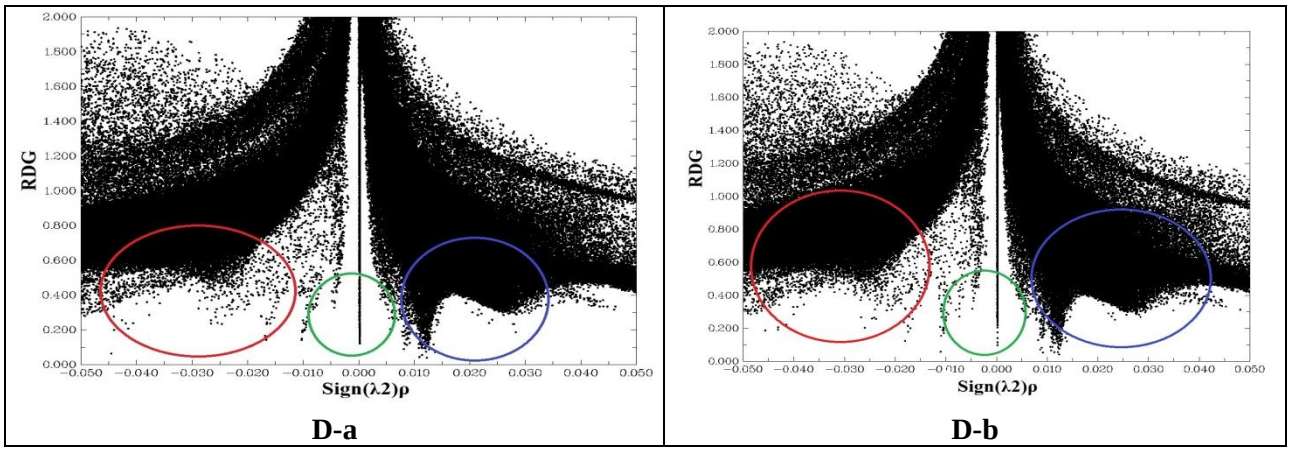

Fig. 5 The RDG Plots of (NH_2NO_2) molecule on the surface of pristine, B, As and B&As doped (4,4) armchair AlNNTs for A-a to D-b adsorption models

In the RDG scatter, graph red color circle shows the attractive interactions, blue color circle denotes strong repulsive interactions and green circle implies low electron density, corresponding to Van der walls interactions. These isosurface are located on the reaction sites of the NH_2NO_2/AlNNTs complex. It clearly observed that in the pristine and As and B&As doped AlNNTs in the A-a, A-b, C-a, C-b, D-a, and D-b models more electron density localized in $\lambda_2<0$ region and the attractive interactions interactions is increase. The results of RDG scatter demonstrate that the interaction of NH_2NO_2 from H head on the surface N atom of nanotube is stronger than other positions, and it is recommended that the pristine and As, B&As doped AlNNTs are a good adsorbent toward NH_2NO_2 molecule. These results are in very good agreement with the thermodynamic and adsorption energies results.

Conclusions

In this study, the DFT methods is utilized to investigate the NH_2NO_2 adsorption characteristic on the surface of pristine, B, As and B&As doped (4, 4) armchair AlNNTs at the B3LYP/6-31G (d, p) level of theory. Inspection of results confirm that the adsorption energy of all models are negative and however the adsorption process of D-a and D-b models is more

stable than other models. The negative values of deformation energy of all models indicate that the molecular curvature is occurred spontaneously from original state. The order of $E^{(2)}$ value for adsorption of NH_2NO_2 from H site is: C-a>A-a>D-a> B-a and from O site is: A-b>C-b>D-b>B-b. The values of $\bigtriangledown^2\rho$ and H_{BCP} for all adsorption models is negative and refers to strong interaction (strong covalent bond) between nanotube/NH_2NO_2. The results of HOMO-LUMO, NBO, AIM, MEP confirm that the charge transfer occurred from NH_2NO_2 molecule toward nanotube. These results are in very good agreement with the thermodynamic and adsorption energies results. The average recovery time of A-a, B-a, C-a and D-a models are 2.07×10^{11} , 2.42×10^{12} , 2.53×10^{13} and 6.05×10^{13} s respectively. These results demonstrate that the interaction between nanotube and NH_2NO_2 at all models is strong, and the pristine and B, As and B&As doped AlNNTs is favorable for making adsorbent of NH_2NO_2 molecule.

Acknowledgment

The author thanks the computational information center of Malayer University for providing the necessary facilities to carry out the research.

Supplementary data

Tables S1– S8 and Figures S1– S12 are given in supplementary data.

References

[1] S. Ijima, Nature. **354**,56 (1991).

[2] V. Derycke, R. Martel, J. Appenzeller, Ph. Avouris, Appl. Phys. Lett., **80**, 2773 (2002).

[3] C. Liu, Y.Y. Fan, M. Liu, H.T. Cong, H. M. Cheng, M. S. Dresselhaus, Science., **286**,1127(1999).

[4] M. Mirzaei, A. Shif, N.L. Hadipour, Chem. Phys. Lett., **461**,246(2008).

[5] M. T. Baei, Monatsh. Chem., **143**,545(2012).

[6] M. T. Baei, A.A. Peyghan, M. Moghimi, S. Hashemian, Superlat. Microstr., **52(6)**,1119(2012).

[7] M. T. Baei, A. A. Peyghan, Z. Bagheri, Struct. Chem., **24(4)**,1007 (2013).

[8] J. Beheshtian, A. A.. Peyghan, J. Mol. Model. **19(6)**,, 2211(2013).

[9] D. Zhang, R. Zhang, Chem. Phys. Lett., **371(3)**,426(2003).

[10] V. Tondare, C. Balasubramanian, S. Shende, D. Joag, V. Godbole, S. Bhoraskar, M. Bhadbhade, Appl. Phys. Lett., **80(25)**, 4813(2002).

[11] Q. Wu, Z. Hu, X. Wang, Y. Lu, X. Chen, H. Xu, Y. Chen, J. Am. Chem. Soc., **125(34)**,10176(2003).

[12] Y. Cao, D. Jena, Appl. Phys. Lett., **90(18)**,182112 (2007).

[13] J. Nipko,C-K. Loong, Phys. Rev. B., **57(17)**,10550(1998).

[14] Z. Zhen, Z. Jijun, C. Yongsheng, S. Paul von Rague, C. Zhongfang, Nanotechnol.**, 18(42)**, 424023 (2007).

[15] P. Ruterana, M. Albrecht, J. Neugebauer, (2003) Nitride semiconductors (handbook on materials and devices. Wiley, New York 2003).

[16] K. H. Khoo, M.S.C. Mazzoni, S.G. Louie, Phys. Rev. B., **69**,201401(2004).

[17] G.Y. Guo, S. Ishibashi, T. Tamura, K. Terakura, Phys. Rev. B., **75**,245403(2007).

[18] C. Attaccalite, L. Wirtz, A. Marini, A. Rubio, Phys. Status. Solidi. B., **244**,4288 (2007).

[19] M. Moradi, N. Naderi, Struc. Chem. **10**,1(2014).

[20] S.F. Rastegar, A. A. Peyghan, H. R. Ghenaatian, N. L. Hadipour, Appl. Surf. Sci., **274**,217(2013).

[21] C. Giordano, I. Ingrosso, M. T. Todaro, G. Maruccio, S. De Guido, R. Cingolani, A. Passaseo, M. De Vittorio, Microelectron. Eng., **86**,1204 (2009).

[22] A. Ahmadi, J. Beheshtian, N. L. Hadipour, Phys. E., **43**,1717(2011).

[23] A. Ahmadi, M. Kamfiroozi, J. Beheshtian, N.L. Hadipour, Struct. Chem., **22**,1261(2011).

[24] Y. Jiao, A. Du, Z. Zhu, V. Rudolph, S.C. Smith, J. Mater. Chem., **20**,10426(2010).

[25. J. Beheshtian, Z. Bagheri, M. Kamfiroozi, A. Ahmadi, Struct. Chem., **23**,653(2011).

[26] A. Ahmadi, N.L. Hadipour, M. Kamfiroozi, Z. Bagheri, Sens. Actua. B-Chem., **161**,1025(2012).

[27] A. Ahmadi, A. Omidvar, N. L. Hadipour, Z. Bagheri, M. Kamfiroozi, Phys., **44**,1357(2011).

[28] J. Beheshtian, M. T. Baei, A. Ahmadi Peyghan, Z. Bagheri, J. Mol. Model., **18**, 4745(2012).

[29] A. A. Peyghan, M. T. Baei, S. Hashemian, P. Torabi, J. Mol. Model., **19**,859(2013).

[30] M. T. Baei, A. A. Peyghan, M. Moghimi, J. Mol. Model., **18**, 4477 (2012).

[31] M. T. Baei, A.A. Peyghan, Z. Bagheri, Chin. Chem. Lett., **23**,965(2012).

[32] J. Beheshtian, H. Soleymanabadi, M. Kamfiroozi, A. Ahmadi, J. Mol. Model., **18**, 2343(2012).

[33] J. Beheshtian, A. A. Peyghan, Z. Bagheri, J. Mol. Model., **19**, 2197(2013).

[34] J. Beheshtian, Z. Bagheri, M. Kamfiroozi, A. Ahmadi, Struct. Chem., **23**,653(2012).

[35] J. Beheshtian, M. T. Baei, A.A. Peyghan, Z. Bagheri, J. Mol. Model., **18(10)**, 4745(2012).

[36] J. Beheshtian, M. T. Baei, Z. Bagheri, A.A. Peyghan, Microelectron. J., **43(7)**, 452(2012).

[37] J. Beheshtian, A. A. Peyghan, Z. Bagheri Phys. E., **44(9)**, 1963(2012).

[38] J. Beheshtian, M. T. Baei, A. A. Peyghan, Z. Bagheri, J. Mol. Model., **19**, 943(2013).

[39] A. Seif, L. Torkashavand, F. Mohammadi, Cent. Eur. J. Chem., **12(2)**, 131(2014).

[40] M. Shahabi, H. Raissi, J. Incl. Phenom. Macrocycl. Chem., **86**, 305 (2016).

[41] Y. Li, Z. Zhou, J. Zhao, Nanotechnol., **19**, 015202 (2008).

[42] L. Wang, C. Yi, H. Zou, J. Xu, W. Xu, Mater. Chem. Phys., **127**, 232(2011).

[43] M. Rezaei–Sameti, S. Baranipour, J. Phys. Theor. Chem. IAU Iran., **14 (3),** 211(2017).

[44] M. Rezaei-Sameti, N. Javadi Jukar, J. Nanostruct. Chem., **7,**293(2017).

[45] M. Rezaei-Sameti, S. Yaghoobi, Comput. Cond. Mater., **3**, 21(2015).

[46] M. Rezaei-Sameti, E. Samadi Jamil, J. Nanostr. Chem., **3**, 1(2016).

[47] R. Ditchfield, W. J. Hehre, J. A. Pople, J. Chem. Phys., **54**,724(1972).

[48] M. W. Schmidt, K.K. Baldridge, J. A. Boatz, S. T. Elbert, M. S. Gordon, J. H. Jensen, S. Koseki, N. Matsunaga, K. A. Nguyen, S. J. Su, T. L. Windus, M. Dupuis, J. A. Montgomery, J. Comp .Chem., **14** , 1347(1993).

[49] D. F. V. Lewis, C. Ioannices, D. V. Parke, Xenobiotica., **24**, 401(1994).

[50] I. Fleming, Frontier Orbitals and Organic Chemical Reactions. (Wiley, New York 1976).

[51] A. E. Reed, L.A. Curtiss, F. Weinhold, Chem. Rev., **88**, 899(1988).

[52] S, Stegmeier, M. Fleischer, P. Hauptmann, Sens. Actuators B Chem., **148**, 439(2010).

[53] R. F. W. Bader, Atoms in Molecules: A Quantum Theory. (Oxford University Press, New York. 1990).

[54] F. Biegler–Konig, AIM2000 designed (University of Applied Sciences, Bielefeld 2001).

[55] Z. Peralta-Inga, P. Lane, J. S. Murray, S. Boyd, M. E. Grice, C. J. O'Connor, P. Politzer, Nano Lett., **3(1)** , 21(2003).

[56] F.A. Bulat, A. Toro-Labbé, T. Brinck, J. S. Murray, P. Politzer P. J. Mol. Model., **16(11),** 1679(2010).

[57] F. A. Bulat, J. S. Burgess, B. R. Matis, J.W. Baldwin, L. Macaveiu, J.S. Murray, P. Politzer, J. Phys. Chem. A., **16(33)**, 8644(2012).

[58] T. Lu, F. Chen, Multiwfn: a multifunctional wavefunction analyzer, J. Comput. Chem., **33**, 580 (2012).